Increasing Carbon Nanotube Forest Density

by

Alexander P. McCarthy

Submitted to the Department of Mechanical Engineering
in partial fulfillment of the requirements for the degree of

Bachelor of Science in Mechanical Engineering

at the

MASSACHUSETTS INSTITUTE OF TECHNOLOGY

June 2014

Signature redacted

Author .....
Department of Mechanical Engineering
May 9, 2014

Signature redacted

Certified by .....
John G. Kassakian
Professor of Electrical Engineering
Thesis Supervisor

Signature redacted

Accepted by .....
Anette Hosoi
Professor of Mechanical Engineering, Undergraduate Officer

Increasing Carbon Nanotube Forest Density

by

Alexander P. McCarthy

Submitted to the Department of Mechanical Engineering
on May 9, 2014, in partial fulfillment of the
requirements for the degree of
Bachelor of Science in Mechanical Engineering

Abstract

The outstanding mechanical, electrical, thermal, and morphological properties of individual carbon nanotubes (CNTs) open up exciting potential applications in a wide range of fields. One such application is replacing the standard activated carbon electrode in electrochemical double layer (EDLC) ultracapacitors with vertically aligned CNT forests (VACNTs). The specific capacitance of an EDLC scales with the specific surface area of the electrodes, thus this research seeks to increase the areal density of VACNTs, as areal density also scales with surface area. VACNT synthesis requires the preparation of a substrate with (typically iron) catalyst nanoparticles (NPs), which become nucleation sites for CNTs. This research was primarily focused on tuning the catalyst/substrate interfacial interactions in order to promote higher NP areal densities. A variety of density-enhancing procedures demonstrated in the literature were combined with a novel method of simultaneous deposition and NP formation in a series of experiments designed to increase CNT density. With these methods, CNT densities of $5x10^{11}$ were achieved, approximately 5 times higher than the standard method for VACNT synthesis.

Thesis Supervisor: John G. Kassakian
Title: Professor of Electrical Engineering

Acknowledgments

I would like to thank Professor Kassakian for welcoming me into his research group over two years ago, and David Jenicek for being an excellent graduate student advisor and lab mate– thank you for the encouragement and advice. I would also like to thank Kurt Broderick for his advice, time, effort, and amusing conversation. I would like to thank my high school teacher Dr. Scholl for inspiring me in my freshman year to explore the field of material science. Lastly, I would like to thank my parents and brother for their encouragment and support.

Contents

List of Figures

Chapter 1

Introduction

Since their invention, there have been hundreds of potential commercial applications proposed for carbon nanotubes (CNTs) due to their highly attractive properties in a wide range of applications. For mechanical applications, CNTs have exception ultimate tensile strength and elastic modulous. For electrical and thermal applications, CNTs have lower electrical and thermal resistivity than copper. Nanotubes also have incredily high aspect ratios (on the order of 10^5). Despite having amazing properties, there are very few commercial products that use CNTs today, and most of these are simple composite materials that take advantage of CNT mechanical properties (sport equipment for example). The barrier limiting more widespread and diverse adoption is one of synthesis. For example, a single CNT is more conductive than a copper wire of the same diameter, so it has been proposed to replace copper interconnects in microprocessors with CNT forests grown right on the chip [1]. The issue is that CNT forests are not 100% dense, and thus are actually less conductive than a copper interconnect of the same size. The same dilemma limits CNTs from being used for its thermal conductivity properties.

Another potential application that could be commercialized if highly dense CNTs could be synthesized is the use of vertically aligned CNT (VACNT) forests as the active electrode material in ultracapacitors. The electrode material of choice for current ultracapacitors is activated carbon, chosen because it has a high surface area and conductivity [2]. A highly dense VACNT electrode would theoretically have even

higher surface area and conductivity. Thus the goal of this research has been to make advancements towards growing VACNT electrodes that can compete with and exceed the capabilities of activated carbon. The focus of this thesis is on developing procedures for sythescizing highly dense VACNTs.

Chapter 2

Background

A VACNT electrode has three parts: the substrate, the catalyst, and the CNT forest. The catalyst is deposited onto the substrate and CNTs are nucleated and grown from the catalyst. There is a wide variety of options for substrate and catalyst selection and preparation before growing the VACNT forest. The following will outline what common materials and methods are used and why.

2.1 Substrate

VACNTs require a substrate from which to grow. Like many nano scale processes, CNT synthesis requires carefully controlled substrate preparation. For this reason, mono-crystalline aluminum oxide (sapphire) and mono-crystalline silicon are a popular substrates, as atomically smooth surfaces have uniform surface chemistry. An alternative to a crystalline oxide substrate is a metallic substrate, which is of more relevance to this research as the substrate for VACNTs in an ultracapacitor doubles as the current collector, which must be as conductive as possible. Nonetheless, densification of VACNTs grown on non-metallic substrates will be discussed as some of these techniques have the potential to be cross-applied to metallic substrate grown VACNTs.

There are several complications to take into account when using a metallic substrate. CNTs are generally grown at high temperature, so in most cases the substrate

must have a high melting point. In the case of this research, a tungsten substrate was used for this reason. The metallic surface should be prepared to be as smooth and uniform as possible.

When working with a metal substrate on the nano scale diffusion becomes a significant effect. The layer of metal catalyst used to nucleate CNT growth is so thin that if deposited directly onto a metal substrate, a significant fraction of it will be absorbed into the metal substrate, inhibiting dense nanoparticle formation (section 2.2). Thus when a metal substrate is used there is a layer of Al_2O_3 deposited onto substrate before the catalyst is deposited. The catalyst will diffuse more slowly through the Al_2O_3 buffer layer than it would through the metal substrate. The layer of Al_2O_3 is thin enough (typically on the order of 10 nm) that it does not significantly reduce the electrical conductivity of the substrate as a current collector.

2.2 Catalyst

The catalyst forms nucleation points for CNTs. Likely the most common catalyst is iron, but nickel and cobalt are also used. To nucleate VACNTs the catalyst must be in the form of distinct nanoparticles spread uniformly across the substrate. There are a number of ways to seed the substrate with nanoparticles. One common way of seeding the substrate with iron, and the method used in this research, is to use a sputterer to deposit a thin layer of iron onto the substrate. The substrate is then heated until the iron becomes mobile enough to de-wet, beading up to form iron nanoparticles, which hold their morphology when cooled. This process is driven by surface chemistry, and the nano scale nature of it makes it especially sensitive to the exact condition of the substrate. This also provides a number of controllable variables which can be used to intentionally affect NP formation and VACNT growth characteristics.

2.3 CNT Growth

A carbon source is required to nucleate and grow CNTs from the catalyst nanoparticles. For VACNT synthesis this carbon source is usually a carbon rich gas delivered in a thermal chemical vapor deposition (T-CVD) chamber. The substrate is reheated in a flowing atmosphere composed of, at a minimum, an inert carrier gas and a carbon feedstock gas. When the carbon feedstock gas comes in contact with the hot catalyst NPs it decomposes, depositing carbon in the NPs. If the conditions are right, the carbon on the surface of the nanoparticle arranges itself into the beginning of a carbon nanotube. As more feedstock gas deposits carbon onto the NP the carbon nanotube grows. There are two modes of CNT growth: base growth and tip growth [3]. Base growthoccurs when the NP stays adhered to the substrate, with the CNT growing up out of it. Tip growth is where the NP actually detaches from the substrate and remains on the tip of the CNT, growing upward with the CNT, while the base of the CNT is adhered to the substrate. Whether base of tip growth occurs depends on how well bonded the NP is to the substrate [4]. VACNT forests can grow up to be millimeters long [5].

The composition of the feedstock also affects the characteristics of the CNT growth. There are a variety of options for feed gas (ethylene, methane, and acetylene are popular. acteylene is used in this research). It is also common to add additional gases which can affect the oxidative state of the NPs and substrate. Common additions include hydrogen and water vapor [5].

Chapter 3

Literature Review

Dense VACNT forests have many potential applications aside from ultracapacitor electrodes, resulting in the literature being full of different techniques for increasing CNT density. This research was primarily driven by creating procedures that combine and innovate upon these techniques to create new procedures that yield high CNT densities. The methods adopted from the literature in this research are based on two basic ideas for increasing CNT density: depositing the catalyst in multiple steps, and altering the Al_2O_3 layer to further inhibit catalyst mobility during NP formation.

3.1 CNT Density Measurement Procedures

There are several common methods used to measure the areal density of VACNTs. A fairly popular method is liquid compaction, in which a forest of VACNTs is wetted with a solvent such as isopropanol which is then allowed to evaporate [6]. As the isopropanol evaporates surface tension forces draw the CNTs together, forming a compacted forest. The degree of compaction, combined with knowledge of average CNT diameter (determined using scanning electron microscopy (SEM) or tunneling electron microscopy (TEM)) is used to derive a theoretical density of the forest based on geometric arguments. It is unclear how accurate this method is, given the idealizations that must be made about VACNT morphology. For this reason a more direct method of measuring CNT density, based on counting defects left on the substrate

when CNTs are removed, was used [7].

3.2 Increased Density through Cyclic Catalyst Deposition

Esconjauregui et. al. [8] observed the size and density of NPs on a substrate depend on the thickness of the catalyst layer, with thinner layers of catalyst forming smaller NPs . In order to create highly dense NPs, Esconjauregui developed a procedure of depositing multiple thin layers of Fe (his catalyst of choice), annealing each layer before the next deposition, with each new layer forming NPs in the spaces between existing NPs. In order to prevent new layers of Fe from simply agglomerating onto already formed NPs, Esconjauregui oxidized each layer of NPs after annealing, forming iron oxide NP. He claims this limited the mobility of the NPs such that they would not combine with subsequent layers of Fe. Esconjauregui validated this theory by demonstrating that substrates with a single layer of 0.5 nm Fe had half NP density of substrates with 2 layer of 0.5 nm Fe. He further claims a CNT density of $1.1x10^{13}$ CNTs/cm^2, measured indirectly with liquid compaction methods (section 3.1). In subsequent experiments Esconjauregui conducted more in depth studies on how the oxidative state of the catalyst controlled bonding to the Al_2O_3 [9], and used transmission electron microscopy to study exactly how catalyst deposited onto existing NPs annealed to form additional NPs in the areas between existing NPs [10].

3.3 Increased Density through Al_2O_3 O_2 Plasma Treatment

Zhong et. al. [11] also uses multiple catalyst depositions to increase NP density, but additionally has developed a procedure to alter the Al_2O_3 layer to further limit the mobility of the catalyst during NP formation . Before depositing Fe (again, the catalyst of choice), Zhong treats the Al_2O_3 layer with an O_2 plasma. He believes

that sputtered Al_2O_3 is porous, and O_2 plasma treatment creates a more fully dense material, which has enhanced Fe mobility reducing properties. To test his theory, Zhong used a range of Fe deposition thickness ranging from 0.3 to 0.7 nm, claiming a maximum CNT density of $1.5x10^{13}$ CNTs/cm^2, measured indirectly with liquid compaction methods. Similar research and results are presented by Fischer in 2011 [12].

Chapter 4

Investigation of CNT Density Dependence on Catalyst Thickness

4.1 Fundamental Challenges of Studying VACNT Synthesis

When proposing to study CNT synthesis, it is important to understand that this system is driven by forces which are numerous, powerful, sensitive, and often poorly understood. Consider for example the forces involved during T-CVD (section ??). The substrate is heated to temperatures as high as 800° C in a gas flow which means thermal conductive, convective, and even radiative forces will be in play. The NPs are so small that surface forces will be dominating, especially at such high temperatures. At the same time the chemistry of the NPs will be rapidly changing as they absorb carbon from decomposing acetylene (C_2H_2) and react with H_2. Infact, the exact mechanism that leads to NPs nucleating CNTs is still debated in the scientific community. Access of the gas flow to the NPs will be driven by viscous and inertial fluid forces, which will depend on the morphology of the VACNTs. The morphology of the CNTs will be changing as the CNTs grow, which affects the temperature, gas concentration, and gas access, meaning that all of these forces are time variant. Dealing with this range of forces would be difficult enough in a macro system, and working

with them on a micro scale is even more challenging. Methods must be more precise to yield reproducible results, and the features of the system require more precise measurement methods to characterize.

4.2 Philosophy and Motivation of Initial Experimentation

Fortunately, there is a large base of literature describing methods that yield reliable VACNT growth. When the research discussed in thesis began, a procedure for reliably growing VACNTs based on the literature base was already developed. Thus, the objective of this thesis was to develop procedures which would increase the density of VACNTs in comparison to this baseline procedure. Even if the densities achieved in this research were not greater than those demonstrated in the most recent literature, these procedures would still demonstrate methods for increasing density. In principle the mechanisms and theories behind the procedures developed can be applied to arbitrary VACNT synthesis systems, and thus still represent a useful contribution to the field. From a big picture perspective, when attempting to improve a system with multiple components (tungsten, Al_2O_3 , Fe, feed gas) and a plethora of variables (time, temperature, pressure, concentration, thickness, ect), it was prudent to select one component and test the effect on the system by varying one variable associated with it. In the early stages of this research the component selected was the Fe catalyst, as it is the component that actually forms the NPs, and the basic goal is to increase NP density. The variable chosen to be altered was the thickness of Fe deposited. Fe thickness was chosen because there is little literature that directly addresses the correlation between catalyst thickness and NP density. Most commonly a thickness of 1 nm is used and cited to grow reliably. It was suspected that varying Fe thickness could result in increasing NP density, becuase it seemed unlikely that the thickness which yielded very reliable CNT density also resulted in the highest NP density, and the odds of a round number (1 nm) thickness being the optimal thickness for optimal

NP density seem low as well. Based on this, substrate were prepared with 0.5, 0.6, 0.8, 1.0, and 1.3 nm of Fe, and test for CNT density after T-CVD.

4.3 Method

4.3.1 Sputtering

Sputtering is a method used to precisely deposit very thin layers of inorganic materials onto substrates. To sputter a material onto a substrate, say Fe onto a tungsten foil substrate, the tungsten is placed in a low pressure chamber with an inert gas atmosphere (in this case Ar), along with a target of pure Fe. Plasma is ignited and localized on the Fe target by magnetic fields. The plasma dislodges monatomic Fe from the Fe target, which then coats the inside of the chamber, including the tungsten foil substrate. The tungsten foil lies on a rotating platen to ensue even coating. In this research sputtering is used to deposit Fe and Al_2O_3 .

Al_2O_3 Deposition

A 7.5 x 50 mm strip of 50 um thick W foil was cleaned and placed in the sputterer (AJA International, Orion Series). The chamber was flushed with Ar for 3 min and brought to a deep vacuum of 5E-4 Torr, before returning the chamber to 3 mT for deposition. The Al_2O_3 gun was slowly brought up to 250 W and allowed to stabilize for 3 min before exposing the substrate. Al_2O_3 was deposited onto a quartz crystal microbalance (with the sample shielded) to determine the deposition rate. This calibration step was performed before the first deposition of any given day. 10 nm of Al_2O_3 was then deposited at 0.15 Å/s.

Fe Deposition

After Al_2O_3 deposition the Fe gun was ignited and held at 110 W for five min in order to burn off any oxide layer that may have formed during storage in air. The Fe gun was then ramped down to 35 W and held for 3 min in order to allow the

deposition rate to stabilize. The same calibration procedure with deposition onto the microbalance was used to determine the Fe deposition rate (also performed before the first Fe deposition of the day). Fe was deposited at 0.1 Å/s. The thickness of the Fe depended on the substrate being prepared.

4.3.2 T-CVD

After the substrate was prepared in the sputterer it was transferred in air to different lab space to where CVD equipment was setup. Square sections (0.75 x 0.75 cm) were cut from prepared substrates and place in T-CVD chamber, with the "deposited—on" side facing down on a silicon heating element (Figure 4-1). The chamber was flushed for 3 min with Ar, and evacuated to to low vacuum. The chamber was then brought to 15 mTorr with 640 sccm Ar, 66 sccm C_2H_2, and 28 sccm H_2). The heating element was brought to 780° C, at approximately 150° C/s. CNTs were allowed to grow in these conditions for 10 minutes, afte r which the heater was deactivated and the chamber flushed with Ar before venting.

4.3.3 CNT Density Measurement

The density of CNTs on the substrate was measured by examining, via SEM, a substrate which has had its CNTs scraped off with a razor blade. When CNTs are scraped off a substrate the NPs that have nucleated CNTs are removed as well, leaving pockmarks that are distinct from NPs (Figure 4-2). SEMs were analyzed using an ImageJ plugin that allowed quick counting of pockmarks.

4.4 Measured CNT Densities

Despite some variation in CNT density within each formulation, there is a clear correlation between thinner Fe depositions and higher CNT density, with the 0.6 nm Fe substrate having a measured density of 1.9×10^{11} CNTs/cm^2 (Figure 4-3, 4-4) Based on this, substrates with even less Fe should yield higher densities; however

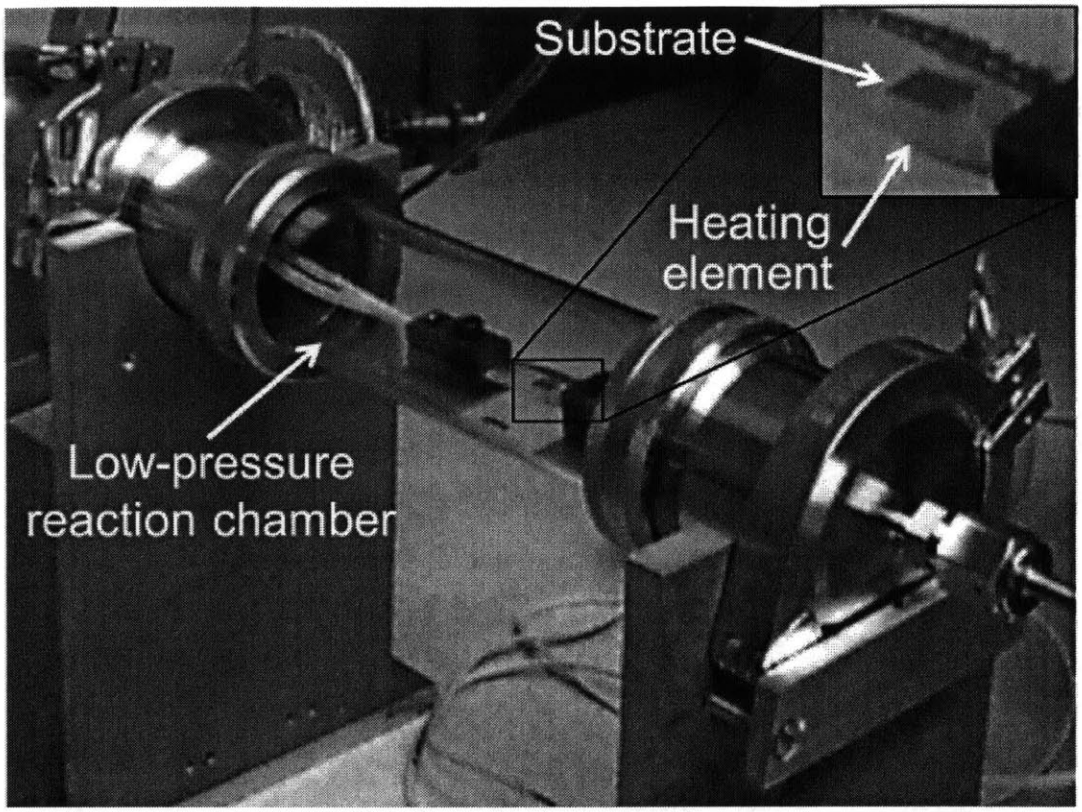

Figure 4-1: T-CVD chamber, with sample on heating element.

there appears to be a limit, as it was impossible to grow CNTs on substrate with less than 0.6 nm Fe. SEMs of these substrates revealed that NPs were not forming during T-CVD. Two theories were developed to explain this. First, the Fe could be too dispersed on the Al_2O_3 such that when it is heated the atoms of Fe are too dispersed to agglomerate and form NPs. Second, the Fe could be adsorbing into the semi porous Al_2O_3 when heated, leaving too little on the surface to form NPs. Regardless the reason, there does seem to be a mechanism that limits NP formation to substrates with greater than 0.5 nm of Fe deposited at room temperature.

4.5 Conclusion

Having started with a reliable substrate preparation and T-CVD procedure with an Fe deposition thickness of 1 nm, VACNTs were also successfully grown on substrates

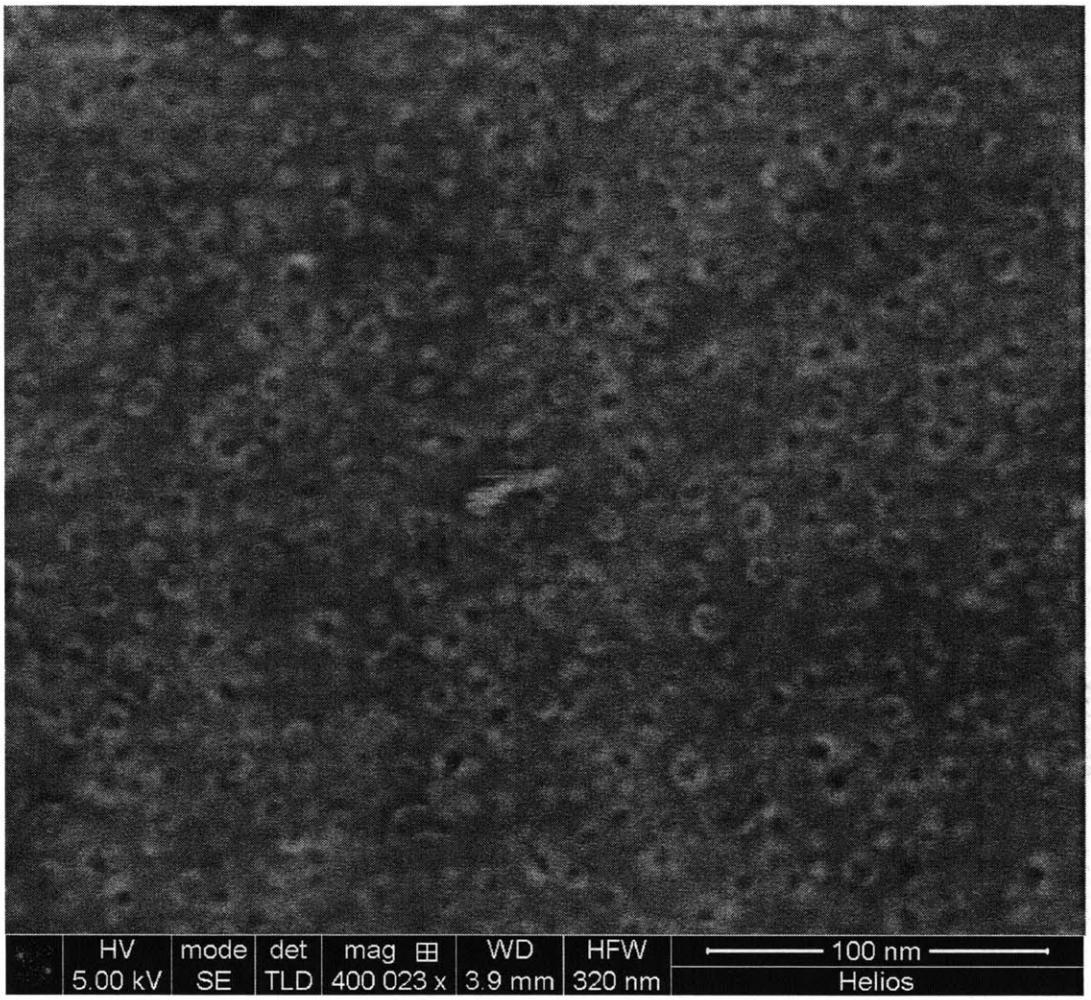

Figure 4-2: SEM of craters left behind on a substrate after CNT removal

with 0.6, 0.8, and 1.3 nm thick Fe layers. SEM analysis revealed that the density is inversely proportional to the Fe deposition thickness. Thus, decreasing Fe thickness is one method to increase CNT density. There is however a limit to this method, as NPs failed to form on substrates with 0.5 nm or less Fe. The process likely causing NP formation failure is adsorption of Fe into the Al_2O_3 , which is discussed in more depth in chapter 7. With more time, these experiments would be repeated to reinforce this relationship, as currently there are only two data points for each substrate type.

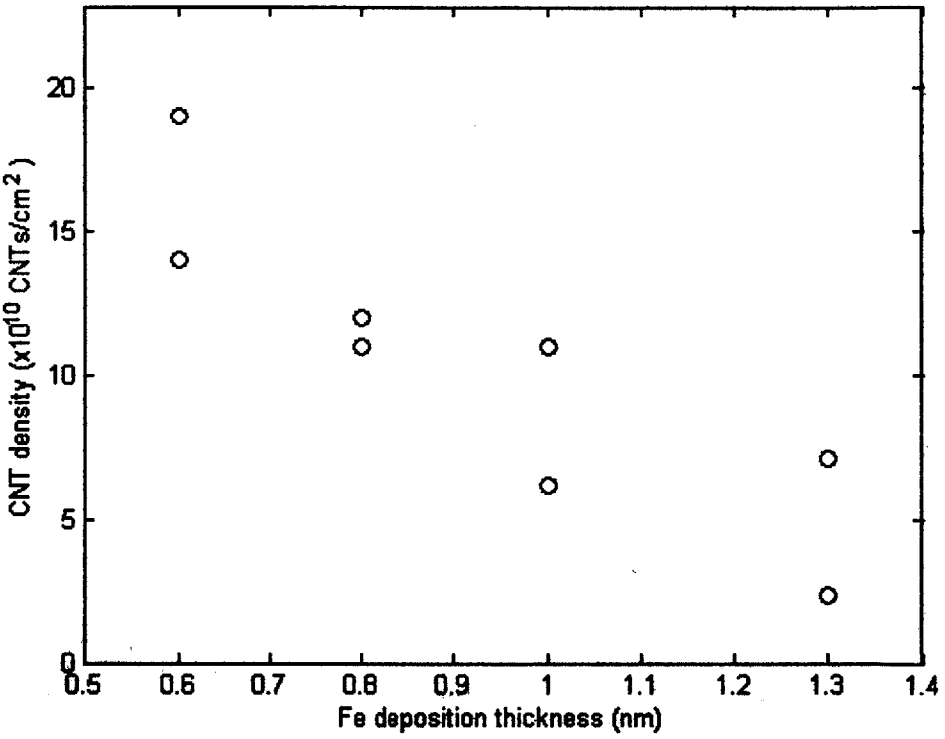

Figure 4-3: CNT densities of substrates with varying thickness Fe depositions.

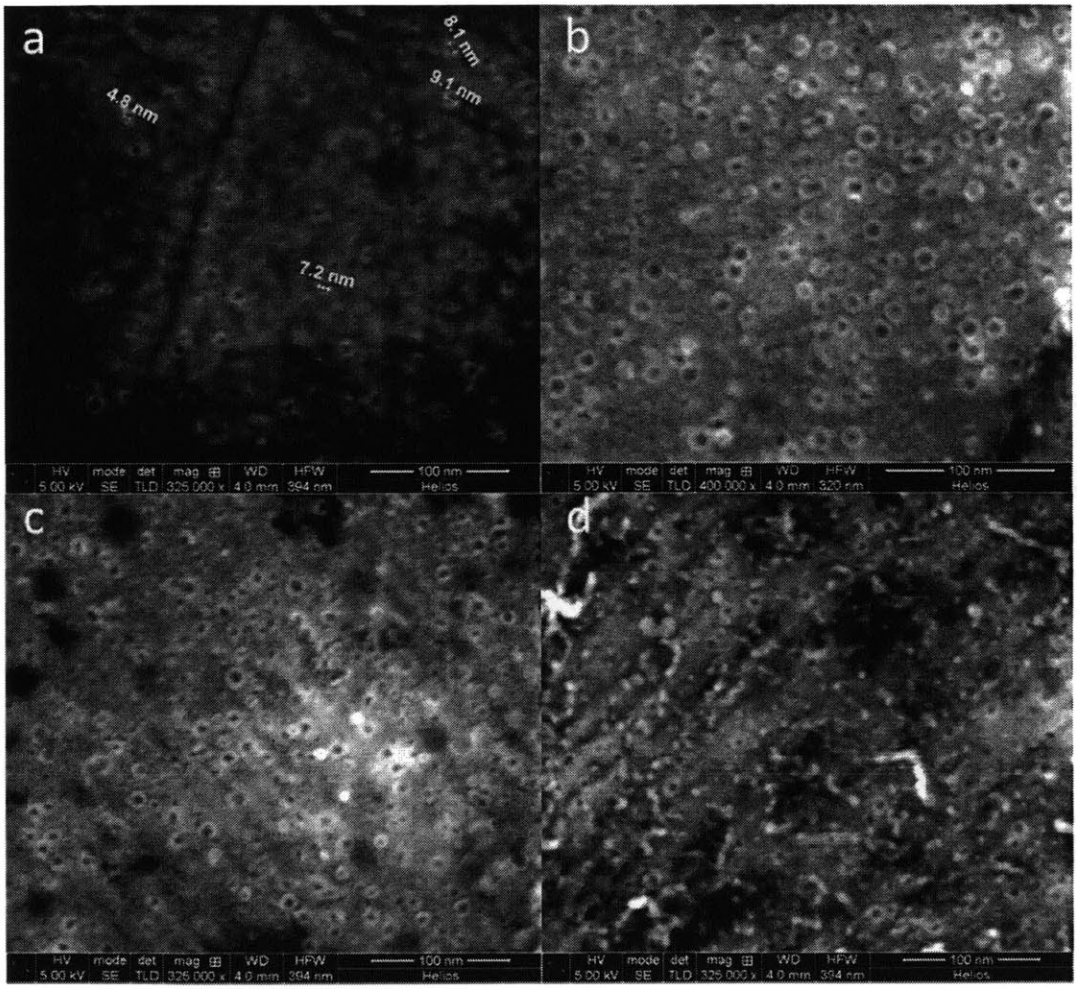

Figure 4-4: SEMs of CNT craters for (a) 0.6 nm Fe room temp dep (b) 0.8 nm Fe room temp dep (c) 1.0 nm Fe room temp dep (d) 1.3 nm Fe room temp dep.

Chapter 5

Cyclic Deposition of Thin Catalyst Layers on a Heated Substrate

5.1 Intro

Experimenting with different layers of catalyst deposition thickness yielded two important results: the density of NPs increases with decreasing catalyst deposition thickness, and there is a limit to how little catalyst can be deposited before NP formation fails to occur. It was additionally observed that while the high density NP substrates, made form deposited 0.6 nm of Fe, were still not fully dense (i.e. there was still room between NPs in which additional NPs would fit. Naively, based on standard methods, to form more NPs, more Fe is required, and if the Fe is deposited all at once, the substrate will be back to having fewer and lower density NPs. A procedure was thus adapted from the literature (section 3.2) to overcome this problem. This new procedure relies on depositing an initial thin layer of Fe, annealing it to form a high density, yet disperse, NP layer, followed by the deposition and annealing of another thin layer of Fe, forming more small NPs in the gaps between existing NPs. In order to keep newly deposited layers of Fe distinct from existing layers, the existing layers are exposed to O_2 after deposition, creating iron oxide NPs. These NPs are less mobile, which theoretically limits Ostwald Ripening and combination with the newly deposited Fe layers [10]. After NP formation, the substrates are treated with a

reducing H_2 plasma to convert the iron oxide back to Fe, so that they can readily absorb carbon during T-CVD and nucleate CNTs. What makes this procedure novel is that the Fe was deposited onto a heated substrate. The theoretical advantage of this procedure is that the substrate spends less time at high temperature, compared to the procedure used in the literature; the literature procedure requires the substrate to be heated to and cooled from the annealing temperature for every deposited layer of Fe. Less time at high temperature theoretically reduces the degree of Ostwald Ripening(a microscale phenomenon driven by surface forces that causes atoms to gradually migrate from smaller particles to larger particles, resulting in only the larger particles remaining) . In this set of experiments three substrates were prepared, one with 2 layers of 0.5 nm Fe (referred to as double dep), one with 3 layers of 0.3 nm Fe (referred to as triple dep), and one with a single layer of 0.5 nm Fe (referred to as single dep).

5.2 Method

5.2.1 Al_2O_3 deposition

Al_2O_3 was deposited onto a tungsten foil substrate in the same manner as described in section 4.3.1.

5.2.2 Fe Cyclic Deposition

After Al_2O_3 deposition the substrate (still inside the sputterer) was ramped to 500° C at 1° /s in an 3 mTorr Ar atmosphere. The Fe gun was burned in and calibrated in the same manner as described in section 4.3.1. Fe was deposited (either 0.3 or 0.5 nm, depending on the substrate being prepared), followed by a one minute exposure to 12 sccm 3 mTorr O_2. The chamber was flushed with Ar, and brought back to 12 sccm 3mTorr Ar. After waiting 1 min for NPs to form (annealing), the subsequent deposition of Fe was preformed following the same procedure. After Fe deposition the substrate was cooled in a 3 mTorr Ar atmosphere to 200° C, after which the sputterer was vented and the substrate was removed.

5.3 H_2 Plasma Treatment

After deposition substrates were transferred in air from the sputterer chamber to a separate plasma treatment chamber. The chamber was evacuated and filled with a 5 sccm mix of 5% H_2 95%. A plasma was lit and maintained for 2.5 minutes at 200 W.

5.3.1 CNT and NP Density Measurement

The CNT density was measured in the same manner as described in section 4.3.3. Additionally, sample of the substrate were analyzed before CVD, in order to measure the density of NPs formed during the cyclic deposition process.

5.4 NP and CNT Densities

If the theory behind this procedure is accurate, the double dep substrate should yield approximately twice the NP density as the single dep substrate, which is what was observed (Figure 5-3). The single dep procedure yeilded NP densities on the order of $8x10^{10}$ NPs/cm^2, while the double and triple dep procedures yielded densites on the order of $25x10^{10}$ and $43x10^{10}$ NPs/cm^2, respectively (Figure 5-1). This indicates that it is possible to deposit and anneal a layer of Fe onto preexisting NPs without agglomerating onto the existing NPs. The trend continues with the triple dep substrate, which had approximately a 4x increase in NP density over the single dep. While the NP densities indicated improvements when using cyclic depositions, the CNT densities of these substrates did not map so simply. During initial experimentation with this procedure a variety of H_2 plasma treatment procedures were tested, until arriving on the one described in section 5.3. Despite this experimentation, the single dep substrate did not grow CNTs. NPs are clearly forming, so for some reason the CNTs did not nucleate on the NPS. The likely culprit is that the oxidative state of the NPs did not favor CNT nucleation. Unfortunately SEM images of this substrate post T-CVD were not taken, otherwise it would possible to see there was a morphological reason for the lack of CNTs. The double dep substrate behaved as

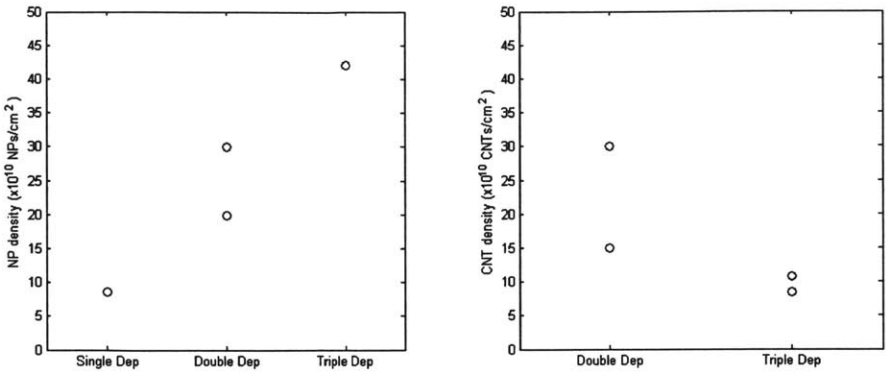

Figure 5-1: NP (left) and CNT (right) densities of substrates with varying cyclic deposition procedure. Points represent values calculated from seperate SEM images of th substrate

expected, with a CNT density equal to the NP density. The triple dep substrate had poor nucleation efficiency (Figure 5-2), resulting in a low CNT density, likely also due to the NPs having an oxidative state that did not favor CNT nucleation.

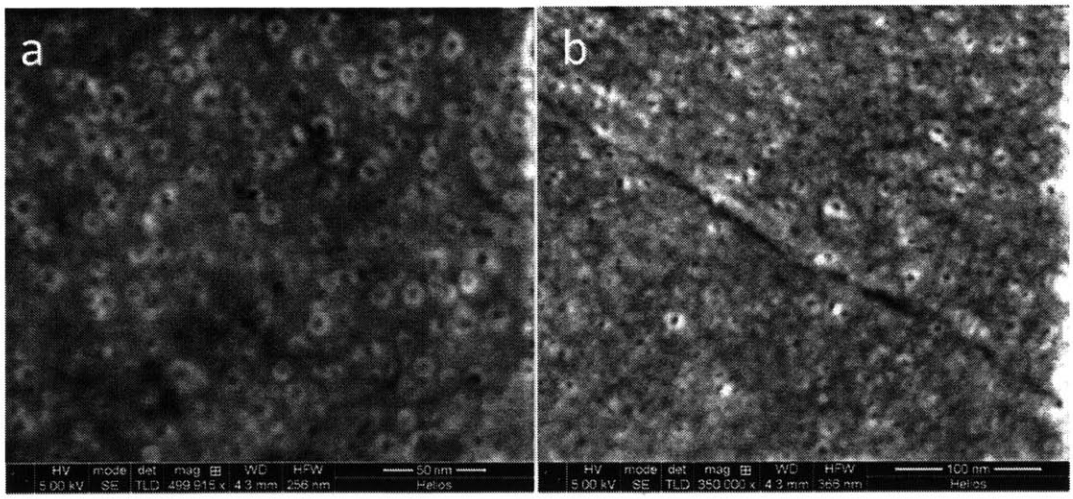

Figure 5-2: SEM of craters for (a) double (b) triple substrates

5.5 Conclusion

This set of experiments brought into light a fundamental challenge when increasing NP density using oxygen immobilization to prevent NP combination: a procedure

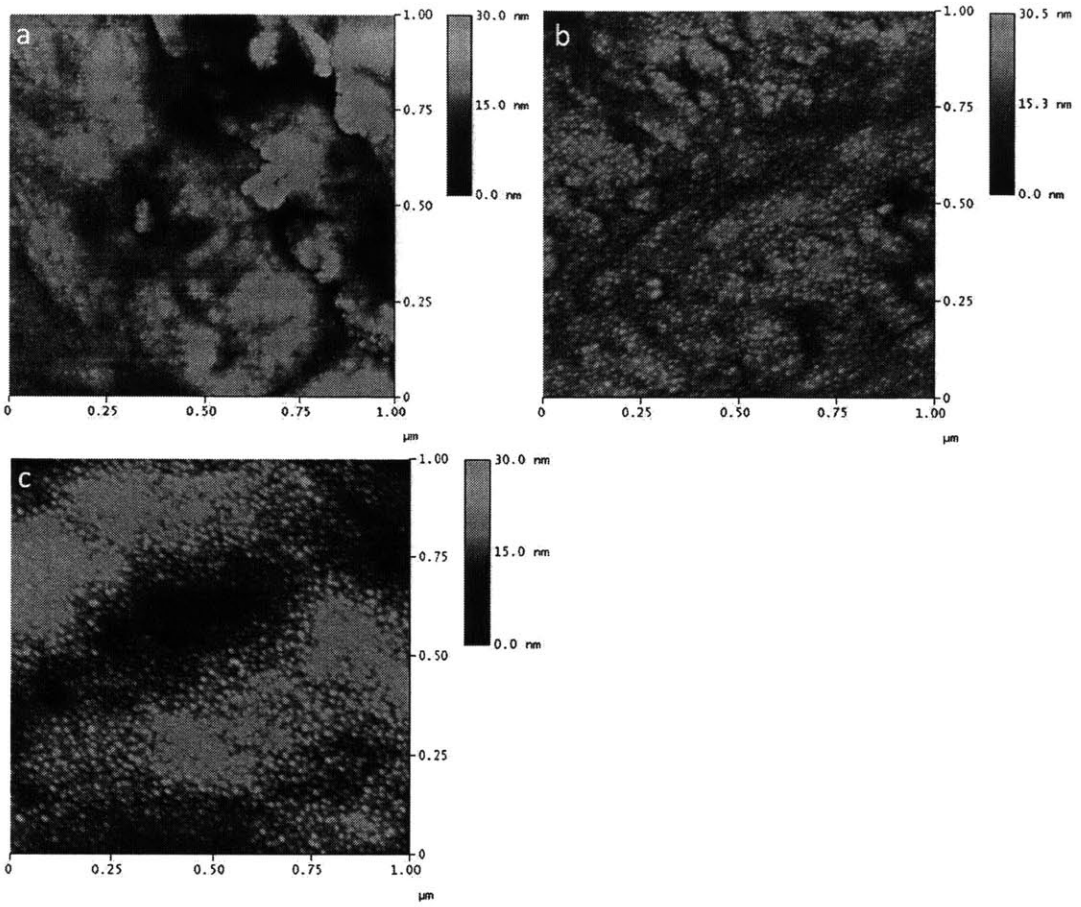

Figure 5-3: AFM of NPs on (a) single dep (b) double dep (c) triple dep substrates, before T-CVD

is needed that both immobilizes the NPs, but at the same time does not alter the chemical state of the NP in such a way as to reduce nucleation efficiency. Despite this, the CNT density of the double dep substrates was higher than any procedure used thus far; it was shown that basic theory behind cyclic depositions is sound.

Chapter 6

Cyclic Deposition of Catalyst without Oxidative Immobilization

6.1 Motivation

Cyclic depositions with an oxidative step to immobilize NPs yielded the highest CNT densities measured so far, however there seems to be a limiting tradeoff between the degree of NP immobilization and CNT nucleation efficiency of NPs. To verify the necessity of the oxidative immobilization step, single dep and double dep substrates were prepared without an oxidative step.

6.2 Methods

Single dep and double dep substrates were deposited in the same manner as described in section 5.2.2, with the exception of the oxygen exposure step between layers during Fe deposition, and the H_2 plasma treatment after Fe deposition. T-CVD was carried out in the same manner as decribed in section 4.3.2.

6.3 NP and CNT Densities

Interestingly the NP densities for both of the non-oxidized single and double dep substrates were even higher than that of the oxidized substrates (Figure 6-1), as measured by AFM (Figure 6-2). The non-oxidized double dep substrate showed a nearly 2x increase in density compared to the non-oxidized single dep substrate, indicating that even without oxidizing the NPs, it is possible to deposit distinct layers of Fe. There must therefore be a mechanism that allows Fe deposited onto an existing

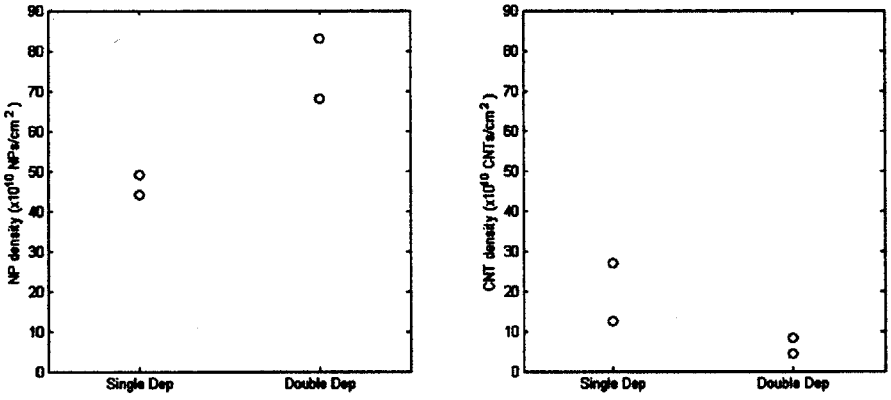

Figure 6-1: NP (left) and CNT (right) densities of substrates with varying cyclic deposition procedures without an oxidation step. Each data point is based on a seperate SEM or AFM of the sustrate.

layer of NP to form seperate NPs. One theory developed is that because the Fe is being deposited onto a hot substrate it is de-wetting and forming NPs immediately, rather than during the 1 min annealing period built into the procedure after each layer of Fe is deposited. This would mean that NPs are being formed from a potentially very thin and discontinuous layer of Fe, as it is actively depositing. If the mobility of the Fe was low enough on the Al_2O_3 , one could imagine NPs forming in the spaces between existing NPs. Additionally, without the oxidation step, the NPs spend 2 minutes less time at high temperature, which potentially reduces the degree of Ostwald Ripening, and increases density.

Despite increasing NP density, the CNT density was actually reduced in comparison to the oxidized single and double dep substrates. (Figure 6-1), as measured via

SEM (Figure 6-3). One theory that could explain this is the Fe deposition temperature (500° C) is high enough to de-wet Fe to form NPs, however it is low enough that Fe is sufficiently immobile, resulting in high NP density, whereas the T-CVD temperature (780° C) is hot enough to mobilize the NPs, resulting in Ostwald Ripening and lower densities. On the positive side, these substrates readily grew tall and uniform VACNTs.

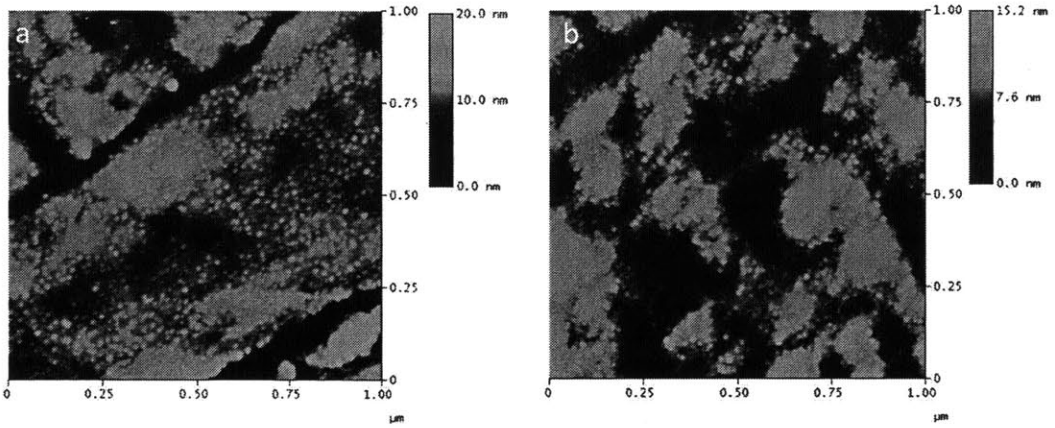

Figure 6-2: AFM of NPs on (a) single dep (b) double dep substrates without O_2 exposure between Fe depositions, before T-CVD

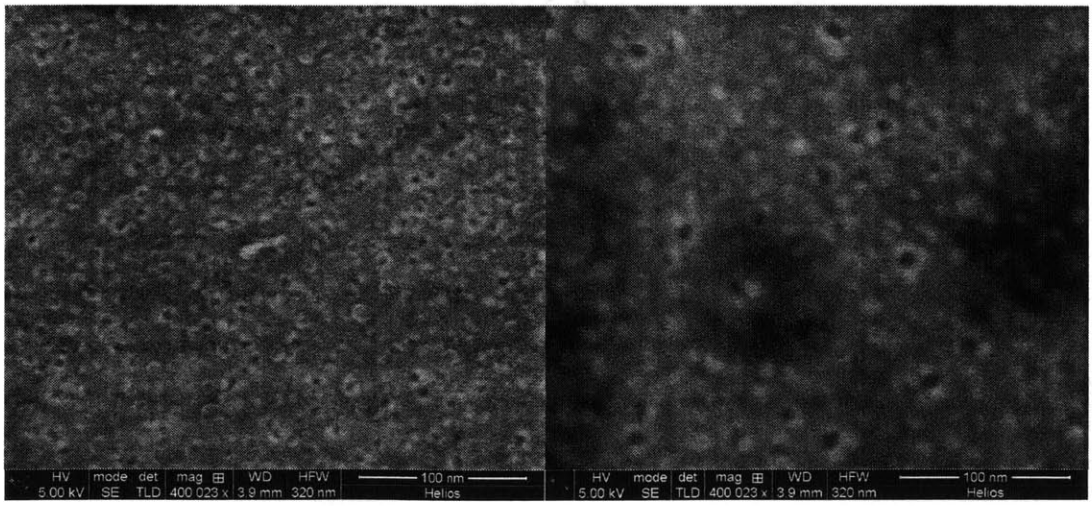

Figure 6-3: SEM of CNTs on (a) single dep (b) double dep substrates without O_2 exposure between Fe depositions, before T-CVD

This conclusion that the oxidative step is actually responsible for reducing mobility

not during deposition, but during T-CVD creates a discrepancy. The oxidative step is supposed to limit mobility by creating iron oxide during deposition, however before T-CVD the iron oxide particles are reduced (theoretically) back to Fe using H_2 plasma. If the particles are reduced before subjecting to T-CVD, then they should agglomerate during T-CVD, as it was postulated they did with the non-oxidized single and double deps. One possible explanation is that when the oxidized NPs are reduced via H_2 plasma, as discussed in chapter 5, they are not fully reduced, and an iron oxide core remains. This iron core anchors the NP to the substrate, and still providing a surface of pure Fe from which CNTs can nucleate (Figure 6-4).

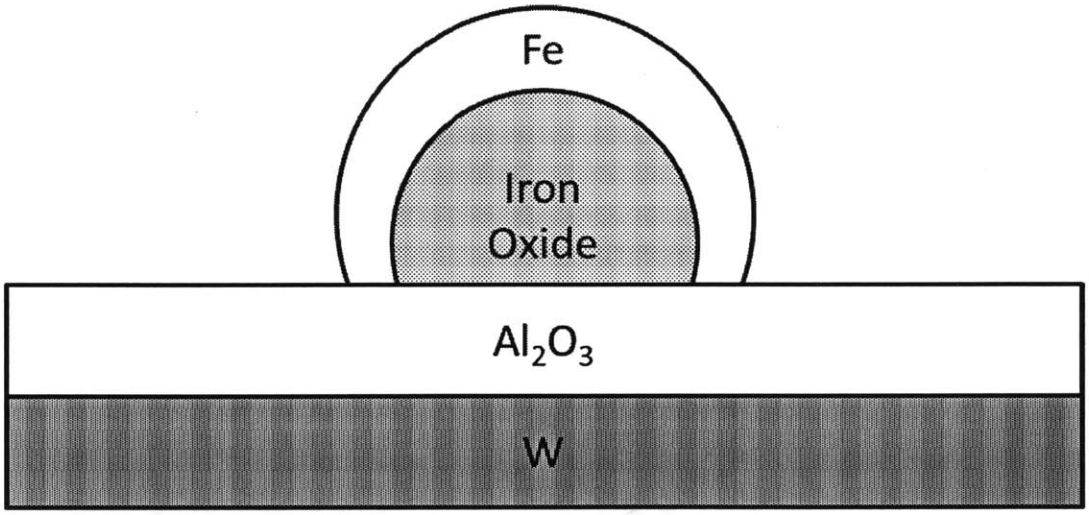

Figure 6-4: Proposed composition of oxidized NP after H_2 plasma treatment

6.4 Conclusion

This set of experiments, in combination with those discussed in chapter 5, seem to indicate that when depositing onto a heated substrate, NP formation actually occurs fast enough to take place during the deposition itself. The oxidative step between Fe depositions, suggested by the literature, is not actually needed to distinguish separately deposited Fe layers, but rather to limit the mobility of the NPs during the heightened temperatures of T-CVD.

Chapter 7

Al_2O_3 modification to reduce catalyst mobility

Based on hot cyclic deps with and without oxygen immobilization, it is clear that limited mobility of the catalyst during heated deposition and T-CVD is required to achieve high CNT density. With substrates prepared thus far, Fe mobility was limited during hot deposition by the nature of the Al_2O_3 /Fe surface interaction [11]. In order to further enhance the mobility limiting properties of the Al_2O_3 a method developed by Zhong was adapted to the hot deposition procedure developed thus far [11]. Zhong has shown that sputtered Al_2O_3 layers are not fully dense, and in this method the Al_2O_3 is treated with an O_2 plasma, which Zhong claims creates a more dense and mobility limiting layer. The goal of this procedure was to enhance the procedure developed in chapter 6 to achieve even higher NP densities. Whether or not this technique would provide enough immobilization to prevent NP Ostwald Ripening during higher temperature T-CVD was unclear. A substrate was prepared with a single 0.6 nm layer of Fe, deposited at high temperature, after the Al_2O_3 layer was O_2 plasma treated.

7.1 Method

Al_2O_3 deposition, Fe deposition, and T-CVD were carried as out in the same manner as described in chapter 6, except between Al_2O_3 and Fe deposition (still at room temperature) the sputterer chamber gas supply was switched from Ar to 30 mTorr 12 sccm O_2. An O_2 plasma was lit in the chamber and maintained at 50 W for 10 minutes, after which the chamber was flushed with Ar and brought back to 12 sccm, 3 mTorr Ar.

7.2 NP and CNT densities

This method of Al_2O_3 modification through O_2 plasma treatement yielded substrate with 0.6 nm of Fe achieving the highest NP density so far measured, with 10^{12} NPs/cm^2 (Figure 7-1). This corroborates with research done by Zhong, [11], demonstrating that Al_2O_3 can be enhanced to further limit catalyst mobility during deposition onto a hot substrate, yielding superior NP densities. Despite this high NP density, the CNT density was only 2.5x10^{11} CNTs/cm^2 (Figure 7-1), implying that while the level of immobilization provided by this Al_2O_3 O_2 plasma treatment method is sufficient to limit Fe mobility at 500° C during NP formation, it is insufficient during the 780° C T-CVD step, resulting in Ostwald Ripening of NPs, and a reduced CNT density, as observed via SEM (Figure 7-2).

7.3 Investigating Effect of O_2 Plasma on Al_2O_3

In early experiments it was found that NPs failed to form when too thin a layer of Fe was deposited. One of the proposed reasons for this was that Fe was being absorbing into the Al_2O_3 . After experimenting with O_2 plasma treated Al_2O_3 substrates and observing significant improvements in NP density, it was theorized that the Al_2O_3 was being densified, as suggested by Zhong [11], resulting in reduced absorption of Fe. To investigate this theory, a method was developed to calculate how much Fe was visible after deposition compared to the originally deposited amount, based on the

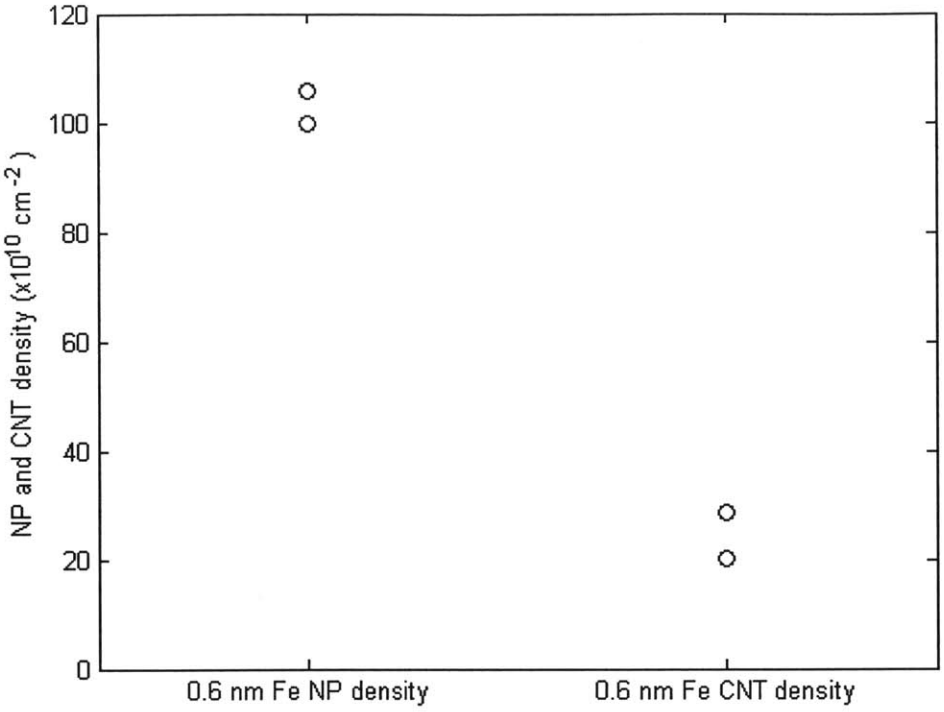

Figure 7-1: NP and CNT densities of substrates with 0.6 nm Fe hot deposited onto an O_2 plasma treated Al_2O_3 layer. Points represent values calculated from seperate SEM images of th substrate

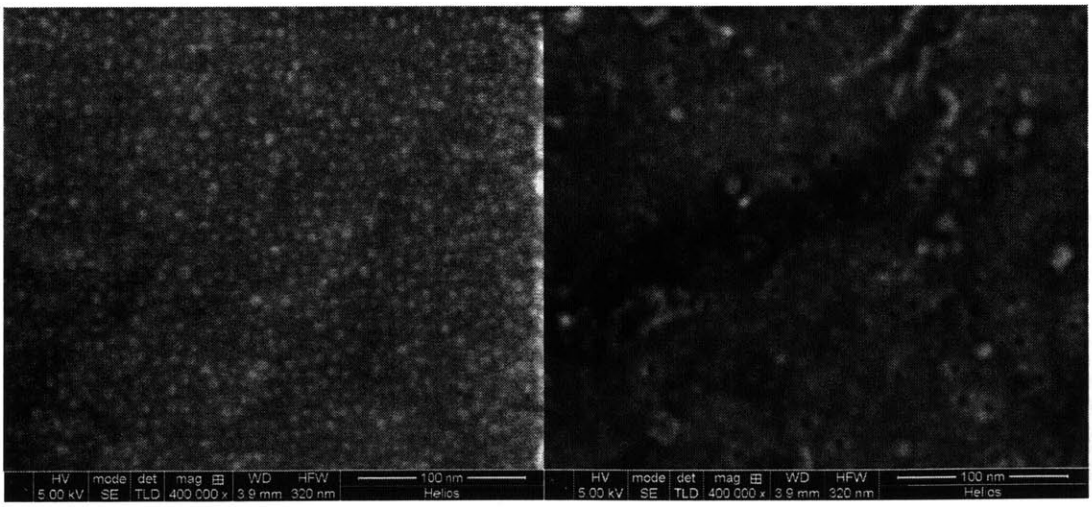

Figure 7-2: SEMs of NP and CNT on substrates with 0.6 nm Fe hot deposited onto an O_2 plasma treated Al_2O_3 layer.

average volume and areal density of NPs.

7.4 Technique

This investigation was based on the notion that it should be possible to derive the volume of deposited iron on a substrate of size A given the average volume of a single NP, V_{NP}, and areal density, ρ, of NPs:

$$V_{deposited} = V_{NP}\rho A \tag{7.1}$$

If it is assumed that an NP has approximately spherical curvature, then volume of the NP can be derived from the radius, r, and the contact angle with the Al_2O_3 , θ (section 9):

$$V = \frac{4}{3}\pi r^3 \sin\left(\frac{\theta}{2}\right)^4 (\cos(\theta) + 2) \tag{7.2}$$

The contact angle of the NPs on the Al_2O_3 was not measured in this experimentation; however it must be greater than 90° because the Fe dewets the Al_2O_3 , rather than wetting. Research done by Kapilasharmi Era shows that for macroscopic droplets of molten Fe on Al_2O_3 the contact angle ranges from 90° to 120° , depending on the Al_2O_3 surface roughness and the atmosphere [13]. While the NPs are not actually molten, the inherent nano scale of the system creates liquid like mobility, and Kapilasharmi found that contact angle was approximately invariant with temperature. Based on this, the contact angle for NPs was estimated to be 105 ± 15° . Using this model, the amount of iron visible after deposition, in the form of NPs, was estimated for a substrate which had an O_2 plasma treated Al_2O_3 layer and 0.6 nm of Fe deposited at 500° C. This was compared to two substrates prepared without O_2 plasma treated Al_2O_3 , one with and 0.5 nm Fe and one with 1.0 nm Fe, both deposited at 500° C.

7.5 Calculated Fe Loss

Using this model and data collected from SEMs about density and size distributions of NPs, a marked difference was observed between substrates with and without O_2 plasma treated Al_2O_3 (Figure 7-3). It is clear that this model is not perfect, as it estimates the amount of visible Fe to be greater than the actual deposited amount for the 0.6 nm Fe O_2 plasma treated Al_2O_3 substrate; however 100% is within the error bounds (calculated based on propogation of uncertainty in NP radius measurement and estimated contact angle) (Figure 7-3). Regardless, it is clear this experiment demonstrates that non O_2 plasma treated substrates are missing Fe, while the O_2 plasma treated substrate appears to have approximately 100% of the deposited Fe forming into NPs (Figure 7-3). One possible explanation for the missing Fe is absorption of Fe into the Al_2O_3 , which, according to Zhong, is porous when sputtered. Whether or not the Fe becomes part of the Al_2O_3 matrix, or if it simply passes through the Al_2O_3 and dissolves into the W substrate is unclear.

7.6 Conclusion

It was demonstrated that Al_2O_3 can be modified by O_2 plasma treatment to yield substrates with Fe deposited at high temperature that yield superior NP densities. The proposed mechanism for this enhancement, based on research done by Zhong in 2012, is a densification of the Al_2O_3 during plasma treatment that creates an enhanced immobilizing Al_2O_3 /Fe interaction. This mechanism is supported by an investigation of how much Fe was absorbed by O_2 plasma treated and non-plasma treated Al_2O_3 substrates, which revealed that plasma treated substrates had significantly less Fe absorption. While this method increased NP densities, relatively low CNT densities were observed, likely due to Ostwald Ripening of NPs during T-CVD, motivating the need for an additional technique to limit NP mobility during T-CVD.

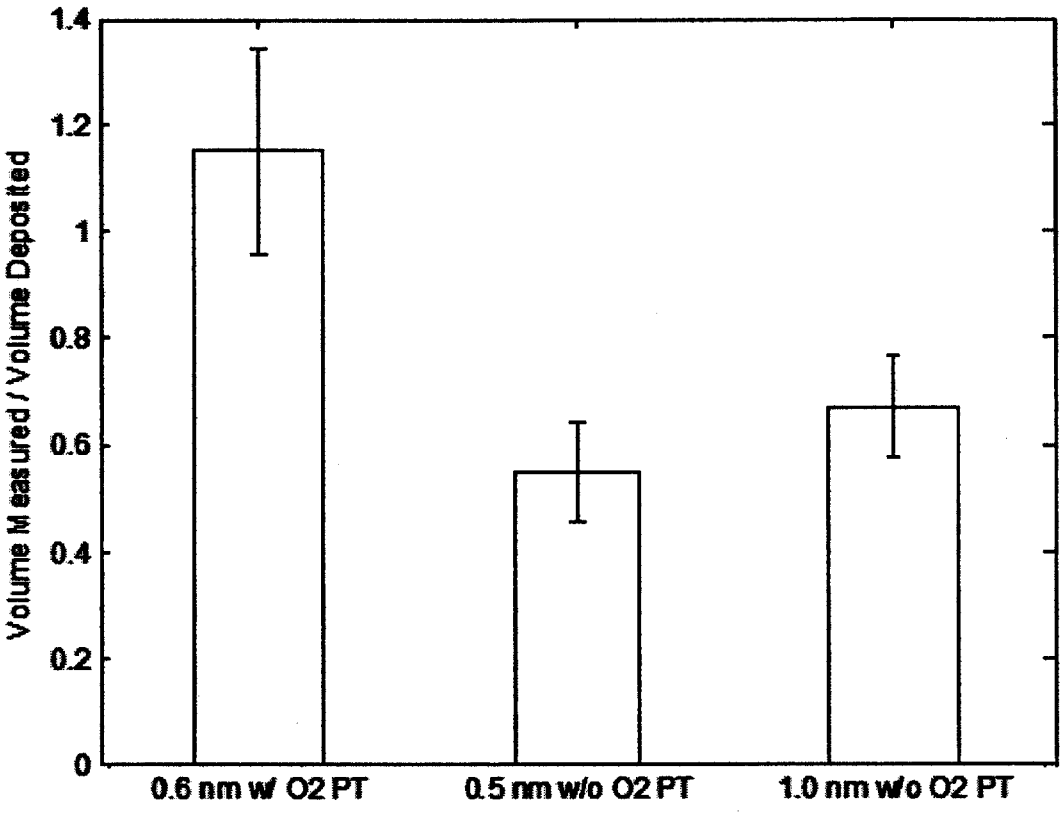

Figure 7-3: Fraction of visible Fe volume in NPs compared to deposited volume for substrate with and without O_2 plasma treated Al_2O_3 , for varying Fe thicknesses, deposited at 500° C.

Chapter 8

Conclusion

A strong correlation was discovered between room temperature deposited Fe catalyst thicknesses, with thin layers (0.6 nm) yielding high VACNT densities and thick layers yielding low VACNT densities. NPs could not be formed for Fe thicknesses less than 0.6 nm, possibly due to adsorption into the Al_2O_3 substrate. This motivated substrates prepared with cyclic depositions of thin layers of Fe on a hot substrate. Initial experiments included an oxidation step between Fe layers in order to immobilize existing NPs before catalyst for subsequent NP layers was deposited. Analysis of NP density for single 0.5 nm Fe substrates and double 0.5 nm Fe substrates indicated that NPs were being formed independently, CNT densities for 0.5 nm Fe double depositions was equivalent to NP densities, indicating that the NPs were not Ostwald Ripening during T-CVD. It was then discovered that even higher NP densities could be achieved by eliminating the oxidative step, although the resulting CNT densities were significantly lower, indicating that Ostwald Ripening was occurring during T-CVD, motivating the argument that an oxidative step is necessary, although perhaps most importantly to immobilize NPs during the high temperatures of T-CVD. Overall, these experiments indicate that to achieve high CNT density, cyclic deposition is necessary, with an immobilization step to prevent NP Ostwald Ripening, most importantly during T-CVD.

This research is ongoing and additional procedures for VACNT densification have been developed, but will not be discussed in depth in this thesis. These include the

immobilization of NPs by depositing a layer of C onto annealing NPs to form iron carbide particles, which, like iron oxide particles, have limited mobility, however they also readily nucleate VACNTs without a reducing plasma treatment. The surface area of a VACNT forest has also been increased after T-CVD by plasma treatment of the forest, which breaks open CNTs, partially exposing the inner surface of the CNTs as well as the outside. These methods are discussed more fully in an upcoming Ph.D. thesis.

Chapter 9

Appendix

If the contact angle of Fe on Al_2O_3 and the radius of an NP can be estimated, then volume of of a single NP can be estimated with the assumption that the droplet has uniform spherical curvature, which minimizes surface energy (Figure 9-1).

$$V = \frac{4}{3}\pi r^3 - \frac{\pi h}{6}(3a^2 + h^2) \tag{9.1}$$

$$\sin(\phi) = \sin(\theta - 90) = -\cos(\theta) = \frac{r - h}{r} \tag{9.2}$$

$$h = r + r\cos(\theta) \tag{9.3}$$

$$\cos(\phi) = \cos(\theta - 90) = \sin(\theta) = \frac{a}{r} \tag{9.4}$$

$$a = r\sin(\theta) \tag{9.5}$$

$$V = \frac{4}{3}\pi r^3 - \frac{\pi(r + r\cos(\theta))}{6}(3(r\sin(\theta))^2 + (r + r\cos(\theta))^2) \tag{9.6}$$

$$V = \frac{4}{3}\pi r^3 \sin\left(\frac{\theta}{2}\right)^4 (\cos(\theta) + 2) \tag{9.7}$$

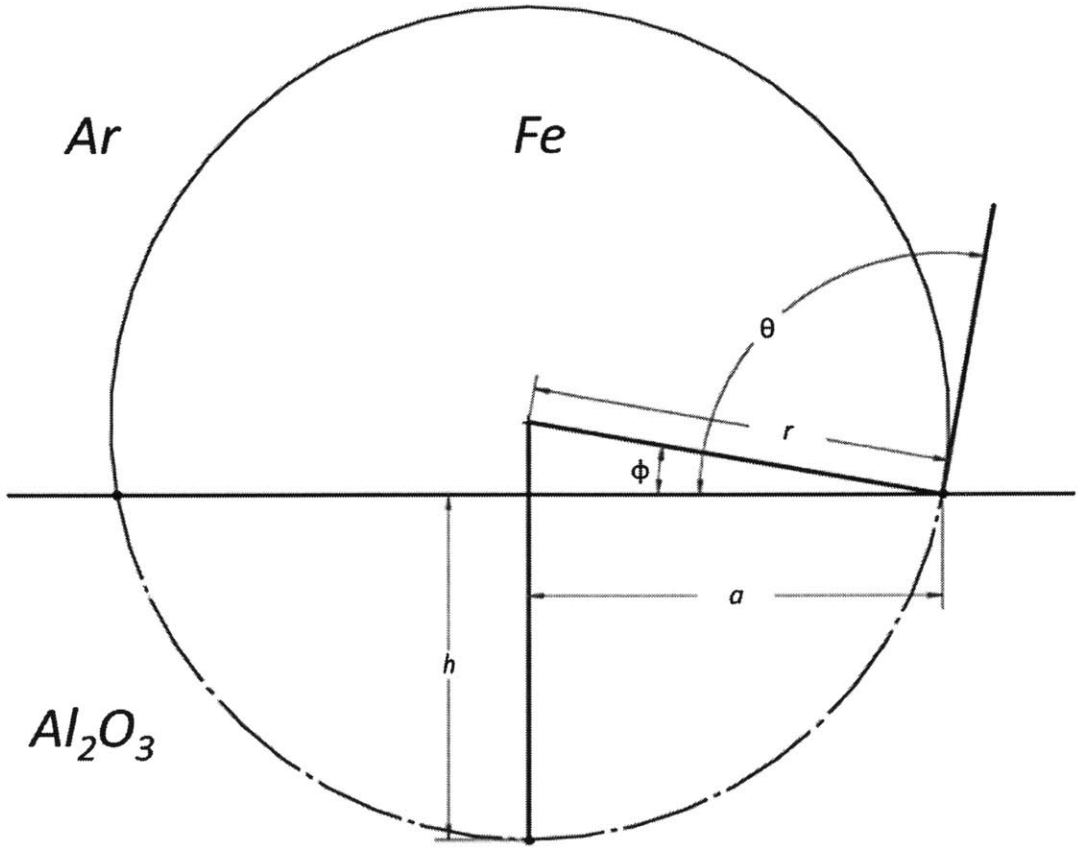

Figure 9-1: Geometry of a non-wetting droplet of Fe on an Al_2O_3 substrate in Ar atmosphere, represented as a partial sphere, where r is the droplet radius, θ is the contact angle, and ϕ, a, and h are parameters used to define the volume of the droplet.

Bibliography

[1] Jun Li, Qi Ye, Alan Cassell, Hou Tee Ng, Ramsey Stevens, Jie Han, and Meyya Meyyappan. Bottom-up approach for carbon nanotube interconnects. *Applied Physics Letters*, 82(15):2491–2493, 2003.

[2] J Gamby, PL Taberna, P Simon, JF Fauvarque, and M Chesneau. "studies and characterisations of various activated carbons used for carbon/carbon supercapacitors". *Journal of Power Sources*, 101(1):109–116, 2001.

[3] Mukul Kumar. *"Carbon nanotube synthesis and growth mechanism"*. PhD thesis, Meijo University, Japan, 2011.

[4] Santiago Esconjauregui, M Fouquet, BC Bayer, S Eslava, S Khachadorian, S Hofmann, and J Robertson. "manipulation of the catalyst-support interactions for inducing nanotube forest growth". *Journal of Applied Physics*, 109(4):044303–044303, 2011.

[5] Kenji Hata, Don N Futaba, Kohei Mizuno, Tatsunori Namai, Motoo Yumura, and Sumio Iijima. "water-assisted highly efficient synthesis of impurity-free single-walled carbon nanotubes". *Science*, 306(5700):1362–1364, 2004.

[6] Don N Futaba, Kenji Hata, Takeo Yamada, Tatsuki Hiraoka, Yuhei Hayamizu, Yozo Kakudate, Osamu Tanaike, Hiroaki Hatori, Motoo Yumura, and Sumio Iijima. "shape-engineerable and highly densely packed single-walled carbon nanotubes and their application as super-capacitor electrodes". *Nature materials*, 5(12):987–994, 2006.

[7] Riccardo Signorelli. "high energy and power density nanotube-enhanced ultracapacitor design, modeling, testing, and predicted performance". 2009.

[8] Santiago Esconjauregui, Martin Fouquet, Bernhard C Bayer, Caterina Ducati, Rita Smajda, Stephan Hofmann, and John Robertson. Growth of ultrahigh density vertically aligned carbon nanotube forests for interconnects. *ACS nano*, 4(12):7431–7436, 2010.

[9] Santiago Esconjauregui, Martin Fouquet, Bernhard C Bayer, Caterina Ducati, and John Robertson. "catalyst design for the growth of highly packed nanotube forests". *physica status solidi (b)*, 248(11):2528–2531, 2011.

[10] Santiago Esconjauregui, Martin Fouquet, Rongsie Xie, Richard Cartwright, Simon B Newcomb, and John Robertson. "catalyst design by cyclic deposition: Nanoparticle formation and growth of high-density nanotube forests". *physica status solidi (b)*, 249(12):2428–2431, 2012.

[11] Guofang Zhong, Jamie H Warner, Martin Fouquet, Alex W Robertson, Bingan Chen, and John Robertson. "growth of ultrahigh density single-walled carbon nanotube forests by improved catalyst design". *ACS nano*, 6(4):2893–2903, 2012.

[12] Caitlin Fisher, ZJ Han, Igor Levchenko, and K Ostrikov. "control of dense carbon nanotube arrays via hierarchical multilayer catalyst". *Applied Physics Letters*, 99(14):143104, 2011.

[13] Era Kapilasharmi. *"Investigation of Interactions between Liquid Iron Containing Oxygen and Aluminosilicate Refractories"*. PhD thesis, 2003.